Journal of Modern Optics
Publication details, including instructions for authors and subscription information:
http://www.tandfonline.com/loi/tmop20

Multidimensional calculation of ray path in a twisted nematic liquid crystal cell

Sung-Ho Youn[a], Byung-June Mun[a], Joun Ho Lee[b], Byeong Koo Kim[b], Hyun Chul Choi[b], Seung Hee Lee[c], Bongsoon Kang[a] & Gi-Dong Lee[a]

[a] Department of Electronics Engineering, Dong-A University, Busan 604-714, South Korea

[b] LG Display Co., Ltd., Gumi, Gyung-buk, 730-731, South Korea

[c] Department of BIN Fusion Technology and Department of Polymer-nano Science and Technology, Chonbuk National University, Jeonju, Jeonbuk 561-756, South Korea

Published online: 06 Feb 2014.

To cite this article: Sung-Ho Youn, Byung-June Mun, Joun Ho Lee, Byeong Koo Kim, Hyun Chul Choi, Seung Hee Lee, Bongsoon Kang & Gi-Dong Lee (2014) Multidimensional calculation of ray path in a twisted nematic liquid crystal cell, Journal of Modern Optics, 61:3, 257-262, DOI: 10.1080/09500340.2013.879939

To link to this article: http://dx.doi.org/10.1080/09500340.2013.879939

Journal of Modern Optics, 2014
Vol. 61, No. 3, 257–262, http://dx.doi.org/10.1080/09500340.2013.879939

Multidimensional calculation of ray path in a twisted nematic liquid crystal cell

Sung-Ho Youn[a], Byung-June Mun[a], Joun Ho Lee[b], Byeong Koo Kim[b], Hyun Chul Choi[b], Seung Hee Lee[c]*, Bongsoon Kang[a]* and Gi-Dong Lee[a]*

[a]*Department of Electronics Engineering, Dong-A University, Busan 604-714, South Korea;* [b]*LG Display Co., Ltd., Gumi, Gyung-buk, 730-731, South Korea;* [c]*Department of BIN Fusion Technology and Department of Polymer-nano Science and Technology, Chonbuk National University, Jeonju, Jeonbuk 561-756, South Korea*

(*Received 11 December 2013; accepted 29 December 2013*)

In general, light propagating an inhomogeneous liquid crystal (LC) cell can be modeled as 'bundle rays' because the LC cell consists of many birefringence layers. In order to calculate the optical path of the propagating light in the inhomogeneous LC cell, we multidimensionally calculated the wavevector, $\boldsymbol{k}$, and the Poynting vector, $\boldsymbol{S}$, of an ordinary and an extraordinary ray at LC grid interfaces, which are isotropic to a uniaxial medium and a uniaxial-to-uniaxial medium, by using the phase matching method. Furthermore, we also investigated the transmission coefficients and transmittance of the ordinary and the extraordinary rays as a function of difference of the optical axes of the facing birefringence medium at the interface to obtain the significant rays in the LC cell. Finally, we could calculate the exact path of the significant rays in the inhomogeneous LC cell, and compared the ray path in an electrically controlled birefringence (ECB) mode and a twisted nematic (TN) LC mode.

Keywords: ray path; Poynting vector; twisted nematic liquid crystal; birefringence; transmission coefficient

1. Introduction

Liquid crystals (LCs) have been used in many optical applications such as polarizers, optical filters, and especially display devices [1–4]. The development of optical technologies using LCs has so far focused on calculating the phase and transmittance of the light in the birefringence layer and at the interface of each material. However, current studies on LCs require ray tracing in each LC layer and at the interface of the LC cell because the latter is currently being developed for use as a ray path-controlling device, such as a tunable lens. Therefore, exact calculation of ray path, in addition to the calculation of the transmission coefficients of the ordinary and the extraordinary waves of the light passing through the LC cell, has become more important.

In order to calculate the ray path of the light in the LC cell, we first need to check the characteristics of the inhomogeneously aligned LC cell. In general, we can model the LC cell, which consists of many birefringence layers whose orientations of directors are changed continuously between neighboring directors in polar and azimuth directions, as being between two isotropic substrates. Therefore, the exact ray position of the light after passing through the LC cell can be obtained after several important calculations, i.e. refraction and reflection at the interface between isotropic and uniaxial birefringence layers, and between inhomogeneous uniaxial-to-uniaxial layers. Moreover, in the case of the LC cell, the ray tracing may be more complicated because the ordinary and extraordinary rays are liable to become bundle rays during passage through the multidimensional structure of the multiple birefringence layers in the cell. Therefore, the calculation of the refraction property as a function of the difference of the director orientation between the neighboring LC molecules is important for simple and exact calculation.

Ray tracing at interfaces between isotropic and uniaxial layers has been studied previously by using several methods, such as Maxwell's equation [5–7], Huygen's principle [8–10], and the phase matching condition [1,11]. The ray path at a uniaxial–uniaxial material interface has also been studied previously [12,13]. However, the methods used gave the solution for the extraordinary ray at only a single interface without change of azimuth orientation of the optical axis. A recent study tried to solve the ray tracing in an arbitrary orientational interface by using Huygen's principle [10]. However, this study also handled only a single interface in the z-direction and it did not calculate the transmission coefficient, so we need to consider the significant rays among the bundle rays in the LC cell for simple and exact calculation.

*Corresponding authors. Emails: lsh1@chonbuk.ac.kr (Seung Hee Lee); bongsoon@dau.ac.kr (Bongsoon Kang); gdlee@dau.ac.kr (Gi-Dong Lee).

In this paper, we have calculated the path and transmission coefficient of the light passing through a multidimensional inhomogeneous LC cell by using phase matching methods. We assumed that the LC cell comprises multiple stacked birefringence layers between two glass substrates. The phase matching in birefringence-to-birefringence interfaces was completed at the z-axis and y-axis in each grid in the LC cell. After calculation of the Poynting vectors of the ordinary and extraordinary rays on the z-axis interface, we checked if the rays in the grid meet the y-axis interface on the grid. In the case where the ray met the y-axis interface, we could deduce the Poynting vectors of two rays by using the dielectric tensor rotation method. We also calculated the transmission coefficients of the light as a function of the difference angles of the orientation director at each interface so that we could obtain significant rays in the LC cell. The LC cell of today has become an important optical device. Therefore, a study regarding this precise calculation for the ray path and the transmission coefficient could make the LC cell become a more-important optical component.

2. Calculation of the path and the transmission coefficient of the light at multidimensional interfaces in LC molecules

In general, the LC cell has two multidimensional interfaces, which are an isotropic–uniaxial (I-U) medium, corresponding to glass substrate to LC molecules, and a uniaxial–uniaxial (U-U) medium, corresponding to LC molecules to LC molecules. Figure 1 shows the relation of the incident and output wavevectors, $\boldsymbol{k}$, at two interfaces at the z-axis interface, which are an I-U medium and a U-U medium. In order to obtain the ray path in the medium, we first need to calculate the Poynting vectors of eigenrays in the media.

In anisotropic media such as LC layers, the electric field, **E**, is not parallel to the dielectric displacement vector, **D,** caused by the dielectric tensor, ε. So, the relation between **D** and **E** can be expressed as $\mathbf{D} = \varepsilon\mathbf{E}$, and the dielectric tensor, ε, in anisotropic media can be represented in an xyz-coordinate system as:

$$\tilde{\varepsilon} = R(\theta,\phi)\varepsilon R(\theta,\phi)^{-1} = \begin{pmatrix} \varepsilon_{xx} & \varepsilon_{xy} & \varepsilon_{xz} \\ \varepsilon_{yx} & \varepsilon_{yy} & \varepsilon_{yz} \\ \varepsilon_{zx} & \varepsilon_{zy} & \varepsilon_{zz} \end{pmatrix} \quad (1)$$

$$R(\theta,\phi) = \begin{pmatrix} \cos\phi & \cos\theta\sin\phi & \sin\theta\sin\phi \\ -\sin\phi & \cos\theta\cos\phi & \sin\theta\cos\phi \\ 0 & -\sin\theta & \cos\theta \end{pmatrix}$$

where $R(\theta, \phi)$ is a rotational matrix and the polar angle, θ, and azimuth angle, ϕ, define the direction of the optical axis of the LC directors. We use the coordinate rotation matrix at the y–z plane to solve the tensor ε because we assume inhomogeneous alignment of the LC layer along the y–z plane on each layer.

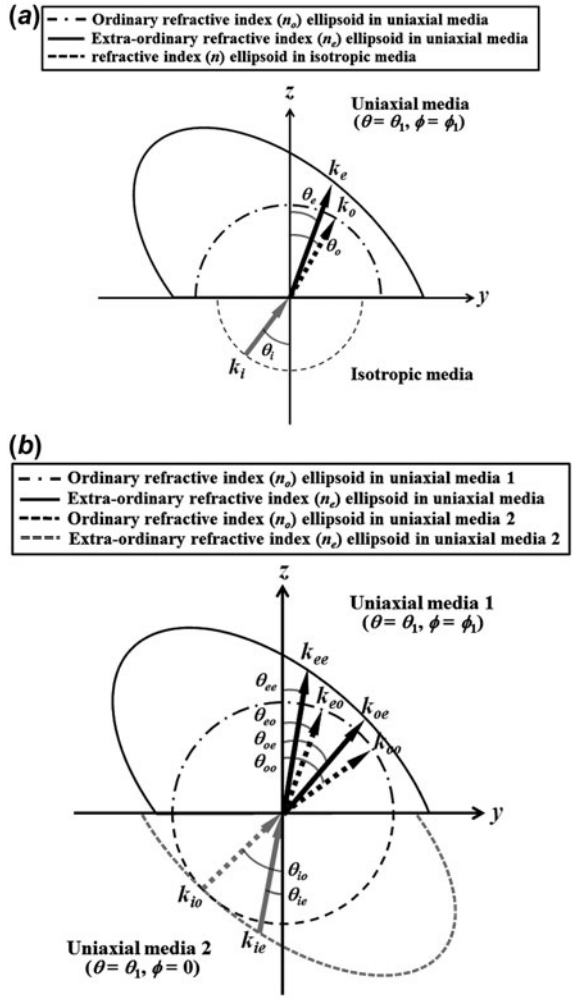

Figure 1. Illustration of directions of the incident and output wavevectors, $\boldsymbol{k}$, at the z-axis interface: (a) an isotropic–uniaxial medium and (b) a uniaxial–uniaxial medium.

In general, the incident light is divided into extraordinary (e) and ordinary (o) waves by birefringence characteristics in the LC cell. The ray path of an o-wave can be easily calculated using Snell's law, as in an isotropic medium. In the case of an e-wave, however, it does not obey Snell's law, so we need to solve the wave equation for calculating the wavevector, $\boldsymbol{k}$, at each interface. Then ray path vector, which means the Poynting vector, $\boldsymbol{S}$, can be obtained as [1]:

$$S = (\sin\theta_e\hat{y} + \cos\theta_e\hat{z})\frac{\sin(\gamma+\alpha)}{\sin(\gamma)} - (\sin\theta\cos\phi\hat{y} + \cos\theta\hat{z}) \quad (2)$$

where θ_e is the angle between the vector $\boldsymbol{k_e}$ and the z-direction, and the γ is the angle between the optical

axis of the LC cell and $\boldsymbol{k_e}$. The value of γ can be calculated using the equation $\cos^{-1}(\sin\theta\,\cos\phi\,\sin\theta_e + \cos\theta\,\cos\theta_e)$. After finding the angle θ_e, therefore, the vector $\boldsymbol{S}$ can be obtained by calculating the angle γ and a dispersion angle α, which is a difference angle between the e-wave vector $\boldsymbol{k_e}$ and vector $\mathbf{S}$, and θ_e.

In this paper, we used the phase matching method for calculating the angle θ_e at two interfaces between I-U birefringence medium and inhomogeneous U-U medium, respectively, as shown in Figure 1(*a*) and 1(*b*).

At an I-U interface, the angle θ_e is easily found from the relation between $\boldsymbol{k_y}$ and $\boldsymbol{k_{ez}}$ as

$$\theta_e = \tan^{-1}\left(\frac{k_y}{k_{ez}}\right) \tag{3}$$

As shown in Figure 1(*a*), the vector $\boldsymbol{k_y}$ is simply calculated at an I-U interface using the equation $n(\sin\theta_i)$, which is the relationship between the refractive index (n) in isotropic media and an incident angle (θ_i) of the incident light. The vector $\boldsymbol{k_{ez}}$ is calculated by using the wave equation that is induced by Maxwell's equation. The wave equation can be simply expressed as two quadratic equations:

$$(k_z^2 - \varepsilon_o + k_y^2)(Ak_z^2 + 2Bk_z + C) = 0 \tag{4}$$

where $A = \varepsilon_{zz}$, $B = \boldsymbol{k_y}\varepsilon_{yz}$, and $C = \varepsilon_{yy}\boldsymbol{k_y}^2 - \varepsilon_o\varepsilon_e$, with ε_{yy}, ε_{yz}, and ε_{zz} given by Equation (1), and ε_o and ε_e are squares of the extraordinary (n_e) and ordinary refractive index (n_o), respectively. The four nontrivial solutions of the vector $\boldsymbol{k_z}$ correspond to transmitted and reflected propagating extraordinary and ordinary waves in the LC cell. Here, two calculated value of the propagating vector $\boldsymbol{k_z}$ can be defined as $\boldsymbol{k_{oz}} = (\varepsilon_o - \boldsymbol{k_y}^2)^{1/2}$ for the ordinary waves and $\boldsymbol{k_{ez}} = [-B + (B^2 - AC)^{1/2}]/A$ for the e-waves.

In the case of the U-U interface in Figure 1(*b*), the refractive index at the interface is changed depending on the incident angle. Therefore, the effective refractive index (n_{eff}) in uniaxial medium 2 of Figure 1(*b*) can be defined as a function of incident angle for calculating of the vector $\boldsymbol{k_y}$. The n_{eff} in uniaxial medium 2 can be calculated using the following equation [11]:

$$n_{eff}(\theta,\phi) = \frac{n_e n_o}{\sqrt{n_o^2 - (n_o^2 + n_e^2)(\sin\theta\cos\phi\sin\theta_e + \cos\theta\cos\theta_e)^2}},$$
$$k_y = n_{eff}(\theta,\phi)\sin\theta_e \tag{5}$$

Finally, we can obtain the angles θ_{ee} and θ_{oe} in Figure 1(*b*) as

$$\theta_{ee} = \tan^{-1}\left(\frac{k_y}{k_{eez}}\right),\ \theta_{oe} = \tan^{-1}\left(\frac{k_y}{k_{oez}}\right) \tag{6}$$

Using the calculated θ_e, the dispersion angle α in the incident plane, which is correlated by vector $\boldsymbol{k_e}$ and the optical axis in the LC cell, can finally be found using

$$\alpha = \tan^{-1}\left(\frac{(\varepsilon_e - \varepsilon_o)\tan\gamma}{\varepsilon_e + \varepsilon_o\tan^2\gamma}\right) \tag{7}$$

From the calculated value of the angle α and the angle γ, we can calculate the Poynting vector $\boldsymbol{S}$ of an e-wave in anisotropic media.

The Poynting vector, $\boldsymbol{S}$, of an e-wave at the y-axis interface can be simply obtained by the dielectric tensor rotation method. Figure 2 shows the relation of the incident and output wavevectors, $\boldsymbol{k}$, at two interfaces at the y-axis interface. In Figure 2, $\boldsymbol{k_{ee}}'$ and $\boldsymbol{k_{oe}}'$ represent, respectively, the 90° rotated wavevectors from the vector $\boldsymbol{k_{ee}}$ and the vector $\boldsymbol{k_{oe}}$ at the y-axis interface. Also, θ_{ee}' and θ_{oe}' in Figure 2 represent the angles between the vector $\boldsymbol{k_{ee}}'$ and the z-direction, and the vector $\boldsymbol{k_{oe}}'$ and the z-direction. Therefore, the angles θ_{ee}' and θ_{oe}' can be obtained by using 90°-rotation values of the dielectric tensor as

$$\tilde{\varepsilon} = R(\theta_r)R(\theta,\phi)\varepsilon R(\theta,\phi)^{-1}R(\theta_r)^{-1} \tag{8}$$

where $R(\theta_r)$ represents the electric tensor rotation matrix and rotation angle θ_r is defined as 90° due to orthogonality between the y-axis and z-axis. After finding the angles θ_{ee}' and θ_{oe}', we can simply calculate the angles θ_{ee} and θ_{oe} at the y-axis interface by rotating 90°.

In this method, Equation (6) for the z-axis interface can also be used at the y-axis interface without any change of equations because the only optical axes in anisotropic media are rotated, so that simple and exact calculation of the Poynting vector is possible. The dielectric tensor rotation method can be applied for

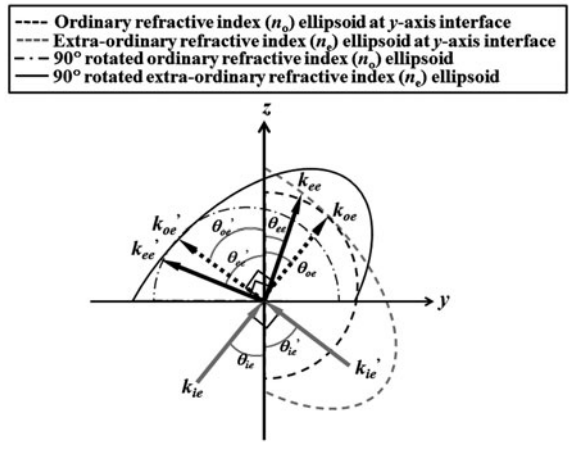

Figure 2. Illustration of rotated direction of incident and output wavevectors, $\boldsymbol{k}$, at the y-axis interface for dielectric tensor rotation.

multidimensional ray tracing in anisotropic media and, thus, we can perform the ray tracing in all LC cells as multiple stacked birefringence layers by applying this method.

Transmittance of the ray at each interface can be also obtained by calculating transmission coefficients of the wavevectors $\boldsymbol{k_o}$ and $\boldsymbol{k_e}$. In order to calculate the transmission coefficients of non-polarized light, we divided the incident light into an *s*-wave and *p*-wave, respectively. Figure 3 shows general ray paths of the *s*-wave and *p*-wave passing through two layers with the difference angle (ϕ_1) of the orientation director with polar angle 45° in anisotropic media at normal incidence. The transmission coefficient of the rays at a uniaxial–uniaxial interface can be obtained by solving the wave equation, so the transmission coefficient of the rays in Figure 3 can be described as

$$t_{ee} = E_{pe1} \cdot E_{pe2} \frac{2n_{eff\_e} \cos\theta_e}{n_{eff\_e} \cos\theta_e + n_{eff\_ee} \cos\theta_{ee}} \quad (9)$$

$$t_{eo} = E_{pe1} \cdot E_{po2} \frac{2n_{eff\_e} \cos\theta_e}{n_{eff\_e} \cos\theta_e + n_{eo} \cos\theta_{eo}} \quad (10)$$

$$t_{oe} = E_{so1} \cdot E_{se2} \frac{2n_o \cos\theta_o}{n_o \cos\theta_{oe} + n_{eff\_oe} \cos\theta_o} \quad (11)$$

$$t_{oo} = E_{so1} \cdot E_{so2} \frac{2n_o \cos\theta_o}{n_o \cos\theta_{oo} + n_{oo} \cos\theta_o} \quad (12)$$

where E_{pe1} and E_{so1} represent the electric field € of e-wave and of o-wave in the first uniaxial layer, and

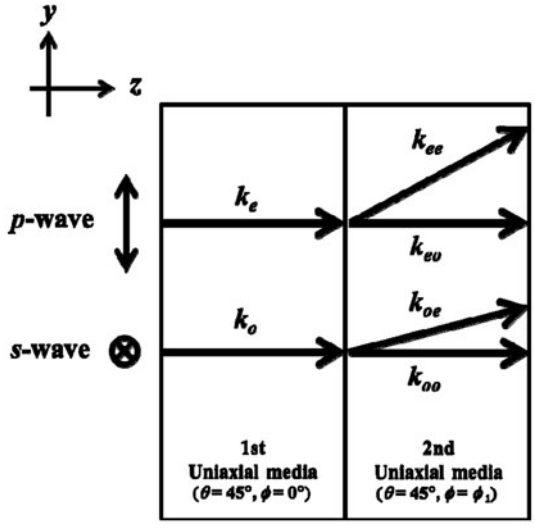

Figure 3. General ray paths of the *s*-wave and the *p*-wave passing through two layers with difference angle (ϕ_1) of the orientation director with polar angle 45° in anisotropic media at normal incidence.

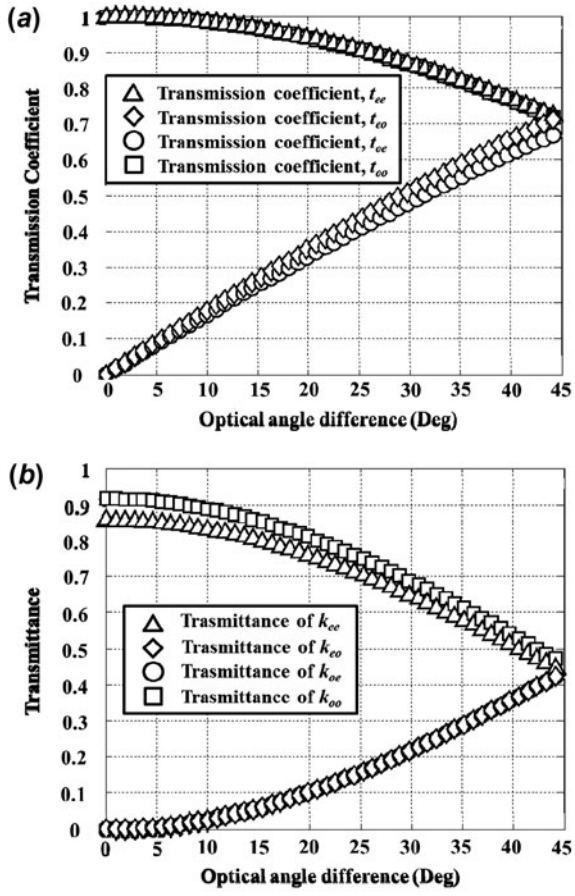

Figure 4. (*a*) The calculated transmission coefficients at interface between first uniaxial and second uniaxial medium, and (*b*) the calculated transmittance of the propagated rays $\boldsymbol{k_{ee}}$, $\boldsymbol{k_{eo}}$, $\boldsymbol{k_{oe}}$, and $\boldsymbol{k_{oo}}$ as a function of the optical angle difference between two birefringence layers.

E_{pe2}, E_{po2}, E_{se2}, and E_{so2} represent the **E** field of *ee*-wave, *eo*-wave, *oe*-wave, and *oo*-wave in the second uniaxial layer.

Figure 4 shows the calculated transmission coefficients and transmittance of the propagated rays $\boldsymbol{k_{ee}}$, $\boldsymbol{k_{eo}}$, $\boldsymbol{k_{oe}}$, and $\boldsymbol{k_{oo}}$ as a function of the optical angle difference between two birefringence layers. In Figure 4(*a*), the e-wave $\boldsymbol{k_e}$ in the first layer is divided into two eigenwaves, $\boldsymbol{k_{eo}}$ and $\boldsymbol{k_{ee}}$, in the second layer. However, the very small optical angle between the two birefringence layers can allow the $\boldsymbol{k_{eo}}$ to be ignored Therefore, in the case of a continuous change of the optical axis for many birefringence layers, such as in the LC cell, its removal from the calculation can make sense. The o-wave $\boldsymbol{k_o}$ in the first layer also is divided into two eigenwaves, $\boldsymbol{k_{oo}}$ and $\boldsymbol{k_{oe}}$, in the second layer. $\boldsymbol{k_{oe}}$ can be also ignored if the optical angle between two birefringence layers is very small. Figure 4(*b*) shows the calculated transmittance, *t*, which is $(\boldsymbol{s}^2 + \boldsymbol{p}^2)^{1/2}$ from Figure 4(*a*).

3. Calculation of the ray path in a LC cell

As we predicted in the ray tracing calculation, the output ray may become a bundle ray after passing through the LC cell. Therefore, we meet a very complex situation for complete calculation of all rays. However, the LC cell can be considered as an optical stack consisting of many birefringence layers and has continuous change of the optical axis between neighboring molecules. For example, a 10 μm cell gap of a twisted nematic (TN) LC cell may contain several thousands of birefringence layers because the LC molecular dimension, normally, is not more than 100 nm. Therefore, we can assume that the difference between the optical axes of the LC molecules never exceeds 0.1°. In this calculation, we can obviously ignore the $\boldsymbol{k_{oe}}$ and $\boldsymbol{k_{eo}}$ in the next layer, so that calculation of the wavevectors $\boldsymbol{k_{ee}}$ and $\boldsymbol{k_{oo}}$ is sufficient for calculation of the significant rays in the LC cell.

From the above approach, we calculated the ray paths of the LC (Merck, MAT-10-566, Δn = 0.2276, n_o = 1.5219, n_e = 1.7495, $\Delta\varepsilon$ = 6.6) cell in an electrically controlled birefringence (ECB) mode (ϕ = 0°) and a TN LC mode (ϕ = 90°). Figure 5(*a*) shows the LC cell structure. The width between electrodes on the bottom substrate is 60 μm and the electrode width is 20 μm. The thickness of the LC layer is 30 μm. Figure 5(*b*)–(*c*) shows the calculated LC director profile of the ECB and TN modes at 8 V. By calculating the director profiles in each gird, we can also calculate the ray path in each grid.

Figure 6(*a*)–(*b*) shows the calculated ray path in the ECB mode and the TN mode. In Figure 6(*a*), the solid lines, which represent the extraordinary rays, are gathering by propagating in the LC layers because of the symmetrical alignment of the LC director along the *y*-axis. It can be observed that the ray path in the ECB mode always stays on the *y*-axis because the azimuth angle ϕ is 0°. The ordinary ray will propagate straightly in the cell because of the isotropic properties of the ordinary medium, and the dotted lines in Figure 6(*a*) represent the ordinary ray in the LC cell. In contrast, the TN LC cell has an azimuth change of the optical axis along the *z*-axis so we can predict that incident rays do not stay on the *y*-axis when propagating in the LC cell.

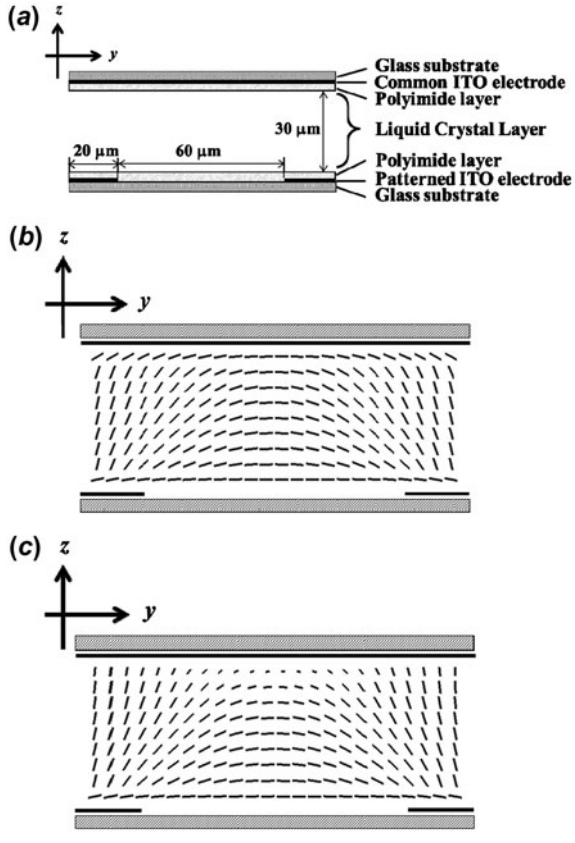

Figure 5. (*a*) The schematic cross section of the LC cell structure for calculation of ray path, and the simulated director profile at the *y*–*z* plane (*b*) in the ECB mode and (*c*) in TN LC mode.

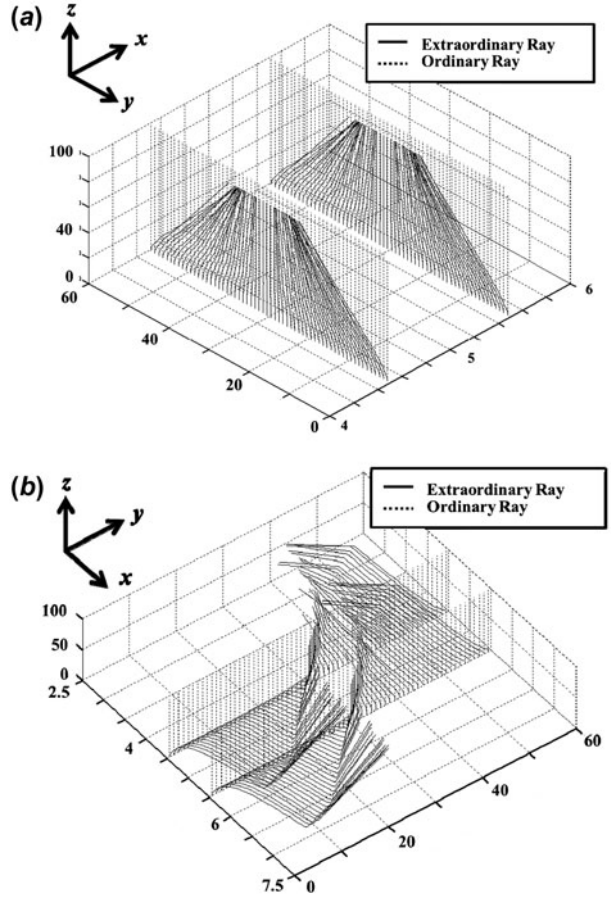

Figure 6. Ray path of the extraordinary and the ordinary waves at normal incidence: (*a*) in the ECB mode and (*b*) in TN LC mode.

Figure 6(*b*) shows the ray path in the TN LC cell. Solid lines represent the ray paths of the extraordinary rays and it can be observed that the rays move not only to the *y*-axis, but also to the *x*-axis because of the azimuth angle ϕ when propagating in the TN LC cell. Dotted lines in Figure 6(*b*) also represent the ordinary rays in the TN LC cell.

4. Conclusion

In this paper, we have calculated the optical path of propagating light in an inhomogeneously aligned LC cell. In order to calculate the inhomogeneous LC layer, we solved the $\boldsymbol{k}$ vector and the Poynting vectors $\boldsymbol{S}$ of an ordinary and an extraordinary ray at the multidimensional interface of birefringence layers with arbitrary aligned optical axes by using the phase matching method. We also investigated the transmission coefficients of the propagating rays in the cell in order to confirm the significant rays in the LC cell. As a result, we could confirm the significant rays in each birefringence layer and could calculate the exact path of the significant rays in the inhomogeneous LC cell. Calculated results were discussed by comparing the ray paths in an ECB LC mode and in a TN LC cell.

Acknowledgement

This research was supported by the Dong-A University research fund.

References

[1] Cojocaru, E. *Appl. Opt.* **1997,** *36*, 302–306.
[2] Yariv, A.; Yeh, P. *Optical Waves in Crystals: Propagation and Control of Laser Radiation*; Wiley, NewYork, **1984;** pp 69–120.
[3] Huard, S. *Polarization of Light*; Wiley: **1997;** Chapter 2.
[4] Lesso, J.P.; Duncan, A.J.; Sibbett, W.; Podgett, M.J. *Appl. Opt.* **2000,** *39*, 592–598.
[5] McClain, S.C.; Hillman, L.W.; Chipman, R.A. *J. Opt. Soc. Am. A.* **1993,** *10*, 2371–2382.
[6] McClain, S.C.; Hillman, L.W.; Chipman, R.A. *J. Opt. Soc. Am. A.* **1993,** *10*, 2383–2393.
[7] Liu, J.-P.; Yau, H.-F.; Ye, Z.; Kuo, C.-H.; Ke, B.W. *Optik (Munich, Ger.)* **2007,** *118*, 147–152.
[8] Avendano-Alejo, M.; Stavroundis, O. *J. Opt. Soc. Am. A* **2002,** *19*, 1668–1673.
[9] Avendano-Alejo, M.; Stavroundis, O. *J. Opt. Soc. Am. A* **2002,** *19*, 1674–1679.
[10] Avendano-Alejo, M. *Opt. Express* **2005,** *13*, 2549–2555.
[11] Liang, Q.-T. *Appl. Opt.* **1990,** *29*, 1008–1010.
[12] Simon, M.C.; Bastida, K.B.; Gottschalk, K.V. *Optik (Munich, Ger.)* **2005,** *116*, 586–594.
[13] Eroglu, A.; Lee, Y.H.; Lee, J.K. *Prog. Electromagn. Res. B* **2013,** *47*, 63–86.